

phys. stat. sol. (a) **114**, 721 (1989)

Subject classification: 78.65; S8.13

*Department of Physics and Meteorology (a) and Materials Science Centre (b)
Indian Institute of Technology, Kharagpur¹*

Optical Properties of CdTe Thin Films

By

S. SAHA (a), U. PAL (a), A. K. CHAUDHURI (a),
V. V. RAO (a), and H. D. BANERJEE (b)

The optical constants (the refractive index n and the absorption constant K) and absorption coefficients α are measured on CdTe thin films in the wavelength range 500 to 2000 nm. Some parameters which affect these optical properties of thin films, such as the film thickness, substrate temperature, doping with impurities like In, BaF₂, PbCl₂ are also investigated. Effective crystallite size and strain are determined by the method of variance analysis of the X-ray diffraction line profiles on the same films. It is observed that there is an increase in optical band gap with decrease in crystallite size and increase in strain.

Die optischen Konstanten (der Brechungsindex n und die Absorptionskonstante K) und der Absorptionskoeffizient α werden in dünnen CdTe-Schichten im Wellenlängenbereich von 500 bis 2000 nm gemessen. Einige Parameter, die diese optischen Eigenschaften dünner Schichten beeinflussen, wie Schichtdicke, Substrattemperatur, Dotierung mit Störstellen wie In, BaF₂, PbCl₂ werden ebenfalls untersucht. Effektive Kristallitgröße und Spannung werden mit der Methode der Varianzanalyse der Röntgenbeugungslinienprofile an denselben Schichten bestimmt. Es wird beobachtet, daß ein Anstieg der optischen Bandlücke mit sinkender Kristallgröße und Anwachsen der Spannung auftritt.

1. Introduction

Cadmium telluride is considered to be one of the most promising materials for the fabrication of solar cell [1, 2]. It has a high absorption coefficient in the visible range of the solar spectrum and its band gap (≈ 1.45 eV) is close to the optimum value for efficient solar energy conversion. A great deal of investigation have been carried out for measuring the optical properties of CdTe films produced by different techniques [3 to 9]. The dependence of optical constants on the conditions of preparation of the films, as well as the nature of doping have also been studied by many groups of workers [4, 10]. The experimental results reported by them show that the values of optical constants are very sensitive to the structure, texture, and impurity contents of the films. But the dependence of optical constants on the particle size of CdTe films deposited on glass substrate have received less attention. The present paper reports the dependence of the optical constants and the band gap on the particle size and composition of the CdTe films deposited on glass substrates under different conditions.

2. Experimental Procedure

Thin films have been prepared from polycrystalline powder of CdTe which has been obtained through direct synthesis of Cd (99.999%) and Te (99.999%) in an evacuated (10^{-4} Pa) graphite-coated quartz tube. The final compound has been confirmed to

¹) Kharagpur 721 302, India.

be CdTe with f.c.c. structure through X-ray analysis. The lattice constant is found to be quite close to the reported value.

Prior to deposition the glass substrates were cleaned with warm chromic acid and distilled water. Thin films of CdTe were deposited on glass substrates by flash evaporation technique under a vacuum of 13.33×10^{-4} Pa. Films of different thickness (200 to 700 nm) were deposited keeping the substrate at room temperature (30 °C). Thickness of the films were maintained almost constant during the deposition of the films at various substrate temperatures (30 to 230 °C). It has been observed that films do not get deposited well on the substrate at substrate temperatures higher than 230 °C. It has been further analysed that the particle size of the films deposited at 230 °C assumes maximum values. Hence the deposition temperature has been optimized at 230 °C at which doping with In, BaF₂, and PbCl₂ has been carried out. A fixed amount of dopant was deposited on to the surface of the CdTe films. The films were then subsequently annealed in vacuum for six hours at a temperature of 150 °C for diffusion of the impurity in the crystallites.

The absorption and transmission characteristics of doped and undoped films were studied by a Simadzu (UV-365) double monochromator recording spectrophotometer. Films were also analysed by an X-ray diffractometer (Philips). Variance and Fourier analysis techniques have been used to estimate the crystallite size and microstrain in cadmium telluride films. The compositions of the deposited films have been estimated through EDX (Camscan Series-II) studies. The average thickness of the films were determined by Surfometer (SF 101). Lattice constants of the films are determined from the X-ray diffraction pattern using a Nelson-Riley plot [11].

3. Results and Discussions

X-ray diffraction patterns show that the CdTe films deposited on glass substrates are polycrystalline in nature with face centred cubic structure. The crystallites are found to be preferentially oriented with (111) face parallel to the substrate [12].

The relation between absorption coefficient α and incident photon energy $h\nu$ [13] can be written for indirect transitions as

$$\alpha h\nu = c_1(h\nu - E_g^i)^2,$$

where c_1 is a constant, E_g^i the indirect band gap. The indirect transition occurs at lower values of α . Accordingly for the smaller values of absorption coefficient $(\alpha h\nu)^{1/2}$ is plotted against the photon energy. The straight-line portions are extrapolated to zero and the values obtained are taken as the absorption edge for indirect transition.

It is assumed that the probability of an indirect transition to occur follows a law $(h\nu - E_g^i)^2$ for a considerable distance in the higher frequency range. Thus the quantity $\alpha_i h\nu$ is calculated in the region of large absorption coefficients, $\alpha_i h\nu$ being subtracted from the measured $\alpha h\nu$. The values of $\{(\alpha - \alpha_i) h\nu\}^2$ are plotted against photon energy. In this region we assume that we are entering the region of direct transitions whose probability follows approximately the relation

$$(\alpha - \alpha_i) h\nu = c_2(h\nu - E_g^d)^{1/2},$$

where c_2 is a constant and E_g^d the direct band gap. Again the extrapolated straight-line intercepts are assumed as the energies for direct transitions.

The $(\alpha h\nu)^{1/2}$ versus $h\nu$ and $\{(\alpha - \alpha_i) h\nu\}^2$ versus $h\nu$ plots for CdTe films of different thickness deposited at room temperature are shown in Fig. 1. It has been observed that the direct band gap decreases with increasing thickness and ultimately comes

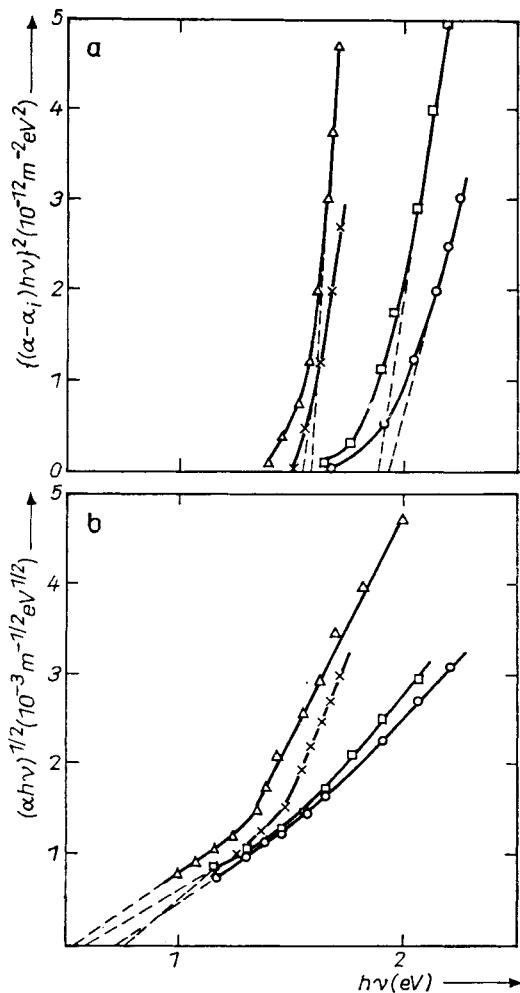


Fig. 1. a) $\{(\alpha - \alpha_i) h\nu\}^2$ vs. $h\nu$ plot and b) $(\alpha h\nu)^{1/2}$ vs. $h\nu$ plot for CdTe films of different thicknesses deposited at room temperature. \circ 200, \square 300, \triangle 400, \times 700 nm

closer to the bulk value when the thickness of the film is large (700 nm). The variation of E_g^d , E_g^i , particle, size microstrain, composition, lattice constant with thickness for films deposited at room temperature is shown in Table 1. It has been found that as the film thickness decreases the tellurium content and microstrain increase, whereas the particle size decreases. The lattice constant increases with the increase of thickness and comes closer to the bulk value when the thickness of the film is large (700 nm). The indirect band gaps are found to differ significantly from the bulk value [14, 15]. According to the band structure of CdTe, calculated by the non-local pseudo-potential method [16, 17] it is unlikely to obtain any indirect optical energy gap less

than the direct band gap value ($\Gamma_{15}-\Gamma_1$). It is known that at lower photon energy transitions the transition rules are relaxed [18] in the presence of a high density of defects, charge impurities, and disorder [19, 20] at the grain boundaries. So the activation energy obtained at lower energies may be due to an internal analog of the Franz-Keldysh effect arising from the electric field developed at the grain boundaries in

Table 1

film thickness (nm)	E_g^d (eV)	E_g^i (eV)	n at 1600 nm	Te/Cd (%)	particle size (nm)	10^4 microstrain	lattice constant (nm)
200	1.94	0.76	2.35	1.610	3.5	160.0	0.6429
300	1.90	0.6	2.50	1.542	4.0	120.0	0.6431
400	1.62	0.56	2.69	1.392	7.5	42.0	0.6443
700	1.56	0.77	2.70	1.145	20.5	35.0	0.6472

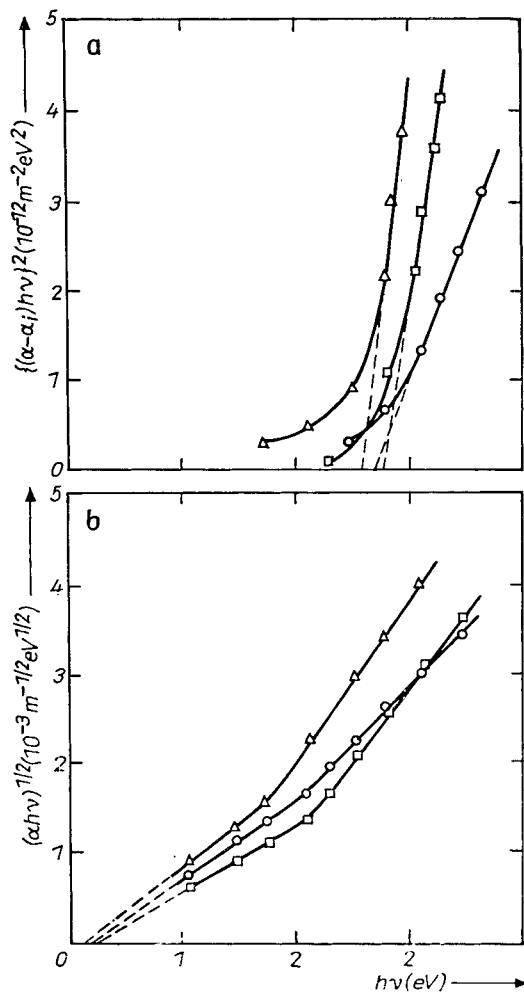


Fig. 2. a) $\{(\alpha - \alpha_i)hv\}^2$ vs. hv plot and b) $(\alpha hv)^{1/2}$ vs. hv plot for films deposited at different substrate temperatures: \square 30, \circ 150, \triangle 230 °C

the materials. Hence this activation energy is due to a process which is different from the indirect transition. After a mathematical separation (deconvolution) of the measured absorption spectra, the direct band gap at lower thickness are found to be higher than the bulk value. However, such variation of band gap with film thickness has not yet been reported in the literature. The increase of E_g^d with decrease of thickness is likely to be attributed to the decrease of particle size, lattice constant, and increase of r.m.s. strain.

Fig. 2 shows the variation of $\{(\alpha - \alpha_i)hv\}^2$ and $(\alpha hv)^{1/2}$ with hv for the films deposited at various substrate temperatures. The film thicknesses are kept nearly constant at 300 nm. The measured values of direct band gaps are found to decrease with the increase

of the substrate temperature. The variation of E_g^d , E_g^i , particle size, microstrain, and lattice constant with substrate temperature are shown in Table 2. It has been observed that as the substrate temperature increases the microstrain de-

Table 2

substrate temperature (°C)	film thickness (nm)	E_g^d (eV)	E_g^i (eV)	n at 1600 (nm)	particle size (nm)	10^4 micro-strain	lattice constant (nm)
30	300	1.90	0.6	2.50	4.0	120.0	0.6431
150	380	1.86	0.58	2.57	8.0	80.0	0.6433
230	300	1.82	0.56	2.61	13.9	60.0	0.6438

creases, whereas the particle size increases. The variations of band gaps are supposed to be due to the change in lattice constant for a considerable change in microstrain.

Fig. 3 shows the variation of $(\alpha h\nu)^{1/2}$ and $\{(a - a_i) h\nu\}^2$ with $h\nu$ for the doped and corresponding undoped CdTe films. The variation of E_g^d , E_g^i , particle size, microstrain, and lattice constant with doping are shown in Table 3. The values of direct band gaps have been observed to be less than that of the undoped film when the films are doped with In and BaF₂. In fact, no appreciable changes could be noticed in films doped with PbCl₂. The decrease of the band gaps can be attributed to impurity absorption in the doped films.

The refractive index n may be computed from the relation [4]

$$n^2 = \frac{n_a^2 + n_g^2}{2} + 2n_a n_g T'' + \left(\frac{(n_a^2 + n_g^2 + 4n_a n_g T'')}{4} - n_a^2 n_g^2 \right)^{1/2},$$

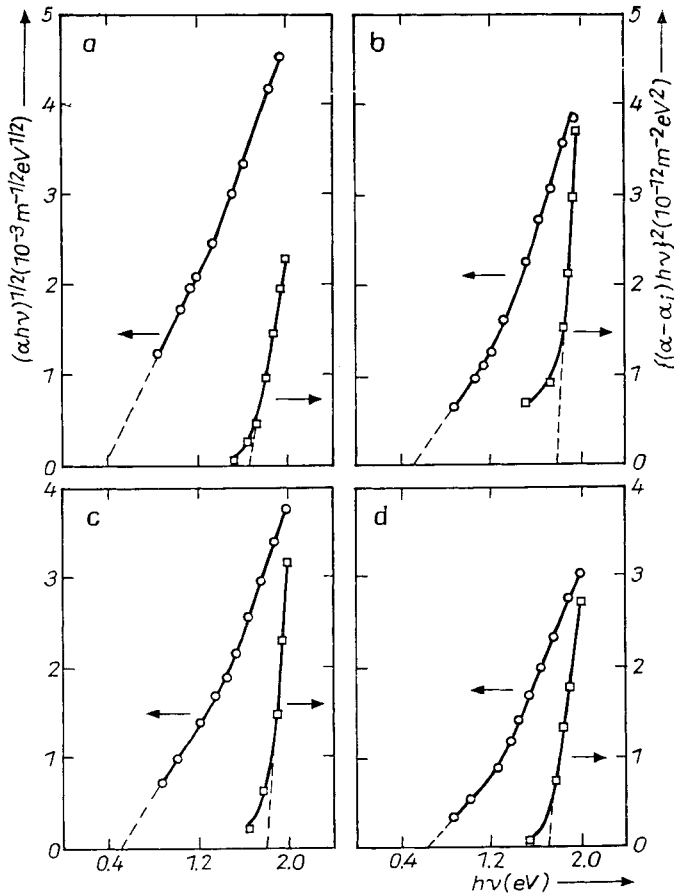


Fig. 3. □ $\{(\alpha - \alpha_i) h\nu\}^2$ vs. $h\nu$ plot and ○ $(\alpha h\nu)^{1/2}$ vs. $h\nu$ plot for films doped with impurities: a) CdTe doped with 4.5 wt% In, b) undoped CdTe, c) CdTe doped with 4.5 wt% PbCl₂, d) CdTe doped with 4.5 wt% BaF₂

Table 3

sample	film thickness (nm)	E_g^d (eV)	E_g^i (eV)	n at 1600 (nm)	particle size (nm)	10^4 micro-strain	lattice constant (nm)
CdTe undoped	300	1.82	0.56	2.61	13.9	60.0	0.6438
CdTe doped with 4.5 wt% $PbCl_2$	300	1.80	0.52	2.48	12.5	61.0	0.6448
CdTe doped with 4.5 wt% BaF_2	330	1.70	0.64	2.59	15.6	52.74	0.6453
CdTe doped with 4.5 wt% In	390	1.68	0.4	2.87	21.8	50.65	0.6473

where

$$T'' = (T_{\max} - T_{\min})/T_{\max}T_{\min}.$$

T_{\max} and T_{\min} represent the envelopes of the maxima and minima positions of the transmittance versus wavelength curve. n , n_a , n_g are the refractive indices of film, air, and glass, respectively.

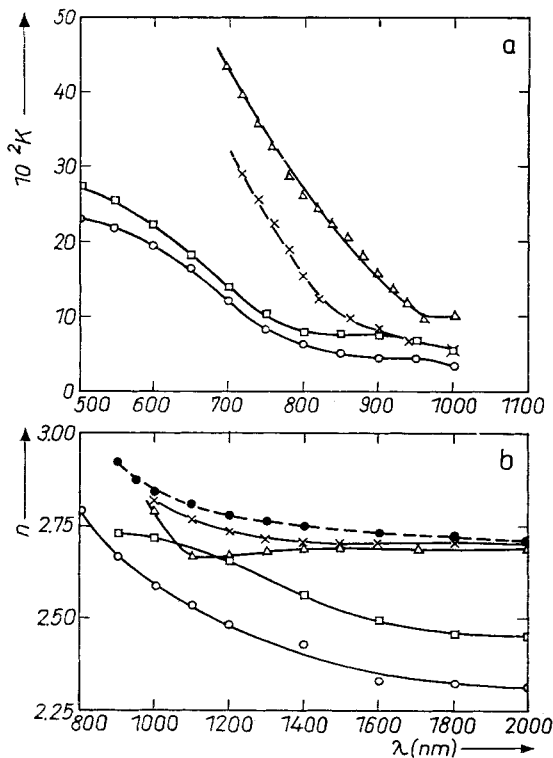


Fig. 4. a) K and b) n vs. λ for CdTe films of different thicknesses deposited at room temperature. \circ 200, \square 300, \triangle 400, \times 700 nm, and --- CdTe single crystal

Fig. 4 corresponds to the variation of refractive index n and absorption constant K with wavelength λ for films of different thickness deposited at room temperature. The refractive index is found to decrease with the increase of the wavelength of the incident photon. At higher wavelength of the incident photon the refractive index (n) tends to be constant. In the region of higher wavelengths it has been observed that n increases with increase of particle size of the film. An unexpected decrease of n has been detected near the absorption edge. Such a decrease of n at short wavelengths has been reported by Manificier et al. [21] for SnO_2 films. He attributed such peculiar variation to the surface effect and volume imperfection on the microscale [22 to 25]. In our case also such a decrease has become more and more prominent as the micro-strain increases in the undoped films. It has been reported that the multiple scattering on microscopic inhomogeneities may lead to serious breakdown of the conventional Kramers-Kronig analysis of reflection and hence transmission spectra [26]. However, in case of thicker films which absorb strongly near and above their absorption edges, the effect of multiple scattering is less and the deviation of n is smaller. A plot of n versus λ for CdTe single crystals [27] is shown by the dashed curve in Fig. 4b. It is observed that the variation of n with λ for CdTe single crystals has a similar trend as for thick films.

Fig. 5 shows the variation of n and K with λ for films deposited at various substrate temperatures. The variation of n with λ is found to follow almost the same trend as that of the bulk materials, for the film deposited at 230°C .

The variations of n and K with λ for doped and undoped films are shown in Fig. 6. It has been observed that for In-doped films n is always greater than for the corresponding undoped film throughout the wavelength region. In case of BaF_2 -doped film n is found to be greater in the lower wavelength region but lower in the higher wavelength region. n is found to be lower in PbCl_2 -doped films than in the undoped films.

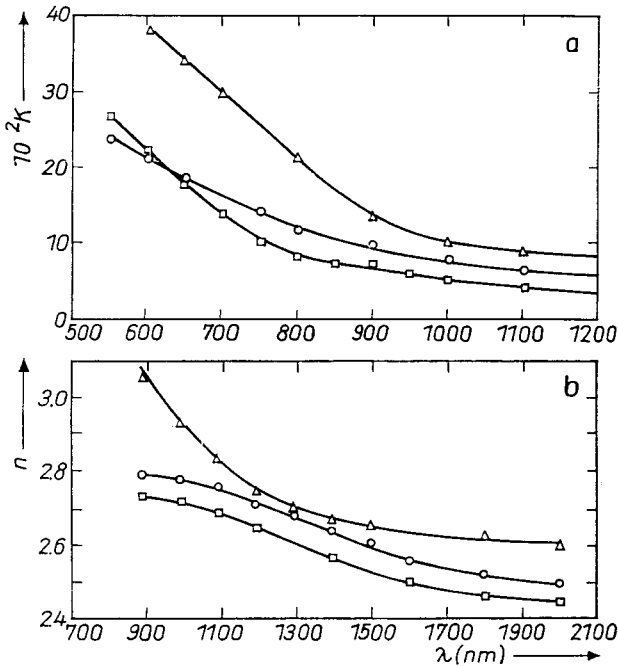


Fig. 5. a) K and b) n vs. λ for films deposited at different substrate temperatures: \square 30°C , \circ 150°C , \triangle 230°C

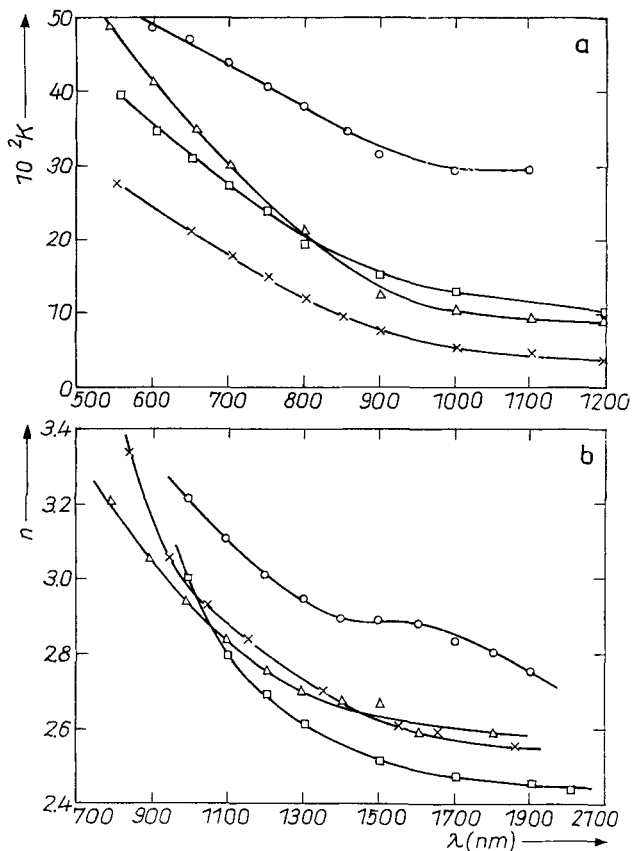


Fig. 6. a) K and b) n vs. λ for films doped with impurities: \square CdTe doped with 4.5 wt% PbCl_2 , \triangle undoped CdTe, \times CdTe doped with 4.5 wt% BaF_2 , \circ CdTe doped with 4.5 wt% In

Acknowledgements

The authors wish to thank the Department of Atomic Energy, Government of India for the financial support and they are also thankful to Prof. D. R. Rao of Materials Science Centre, Indian Institute of Technology, Kharagpur for the spectrophotometer traces.

References

- [1] J. L. LOFERSKI, *J. appl. Phys.* **27**, 777 (1956).
- [2] M. RODOT, *Rev. Phys. appl.* **12**, 411 (1977).
- [3] M. TAKAHASHI, K. VOSAKI, and H. KITA, *J. appl. Phys.* **55**, 3879 (1984).
- [4] S. CHOUDHURI, S. K. DAS, and A. K. PAL, *Thin Solid Films* **147**, 9 (1987).
- [5] F. WANG and D. K. REINHARD, *J. appl. Phys.* **55**, 3702 (1984).
- [6] T. C. ANTHONY, A. L. FAHRENBRUCH, and R. H. BUBE, *J. Vacuum Sci. Technol.* **A2**, 1296 (1984).
- [7] N. MATSUMURA, T. OHSIMA, J. SARAIC, and Y. YODOGUVA, *J. Crystal Growth* **71**, 361 (1985).
- [8] S. GONGOI and K. BARUA, *Thin Solid Films* **92**, 227 (1982).
- [9] B. J. FELDMAN, J. L. BOONE, and T. V. VAN DOREN, *Appl. Phys. Letters* **38**, 703 (1981).
- [10] A. EL-SHAZLY and H. T. EL-SHAIR, *Thin Solid Films* **78**, 287 (1981).
- [11] J. NELSON and D. RILEY, *Proc. Phys. Soc.* **57**, 160 (1945).
- [12] S. SAHA, U. PAL, B. K. SAMANTHARAY, A. K. CHAUDHURI, and H. D. BANERJEE, *Thin Solid Films*, to be published.

- [13] P. W. DAVIS and T. S. SHILLIDAY, *Phys. Rev.* **118**, 1020 (1960).
- [14] D. T. F. MARPLE, *Phys. Rev.* **150**, 728 (1966).
- [15] B. SEGALL, *Phys. Rev.* **150**, 734 (1966).
- [16] M. L. COHEN and T. K. BERGSTRESSER, *Phys. Rev.* **141**, 789 (1966).
- [17] P. S. KIREEV, *Semiconductor Physics*, Izd. Mir, Moscow 1974 (p. 170).
- [18] J. E. LEWIS, *phys. stat. sol. (b)* **143**, 307 (1987).
- [19] D. REDFIELD and M. A. AFROMOWITZ, *Appl. Phys. Letters* **11**, 138 (1967).
- [20] J. D. DOW and D. REDFIELD, *Phys. Rev. B* **1**, 3358 (1970).
- [21] J. C. MANIFACIER, M. DE MUCIA, J. P. FILLARD, and E. VICARIO, *Thin Solid Films* **14**, 127 (1977).
- [22] J. M. PAWLIKOWSKI, *Thin Solid Films* **127**, 39 (1985).
- [23] EHSAN KHAWAJA and S. G. TOMLIN, *J. Phys. D* **8**, 581 (1975).
- [24] H. E. BENNETT and J. M. BENNETT, *Phys. thin Films* **4**, 3 (1967).
- [25] P. ROUARD and A. MESSEN, *Progr. Optics* **15**, 79 (1977).
- [26] I. FILLIŃSKI, *phys. stat. sol. (b)* **49**, 577 (1972).
- [27] D. T. F. MARPLE, *J. appl. Phys.* **35**, 359 (1964).

(Received July 25, 1988; in revised form January 23, 1989)